LA-UR-04-4813

Approved for public release; distribution is unlimited.

Title: EQUATION OF STATE EXPERIMENTS IN EXTREME MAGNETIC FIELDS

Author(s): D. G. Tasker, J. H. Goforth, H. Oona, C.M. Fowler, P. A. Rigg, D. Dennis-Koeller, D. B. Hayes,

Submitted to: The Xth International Conference on Megagauss Magnetic Field Generation and related topics
July 18-23, 2004

Los Alamos
NATIONAL LABORATORY

EQUATION OF STATE EXPERIMENTS IN EXTREME MAGNETIC FIELDS*

D. G. Tasker[1], J. H. Goforth[1], H. Oona[1], C.M. Fowler[1], P. Rigg[1], D. Dennis-Koeller[1], Dennis Hayes, [1]University of California, Los Alamos National Laboratory, [2]Sandia National Laboratory, U.S.A.

Abstract

Transient magnetic fields in excess of ~500 T, with sub-microsecond risetimes, may be used to isentropically compress materials to megabar pressures, opening the way to some fascinating high pressure physics experiments. Isentropic compression experiments (ICE) have been reported by Asay [5] and others, who used a fast, high voltage capacitor bank to provide the necessary current drive. We have adapted our high explosive pulsed power (HEPP) methods to perform the same experiments with a simple and compact HEPP apparatus. In recent experiments we have successfully obtained accurate isentropic equation of state (EOS) data in the Mbar range (i.e., >100 GPa) with our HEPP system. To that end, ICE requires relatively fast risetimes (>10 TA/s in 1.27-cm wide loads over ~500 ns) for HEPP in the loads of interest. It has been a significant challenge to develop the necessary explosive opening and closing switches, which can operate with a few tens of ns precision, to obtain these current risetimes. We will close by describing the EOS data analysis, which is particularly interesting because of the ramp-like nature of the compression waves in ICE experiments.

INTRODUCTION

Transient, high pressure isentropic compression experiments have been of great interest to the high magnetic field community since the early 1970s, as reviewed by Fowler [1]. For example, various teams have sought to metalize liquefied or solidified gasses by shock-free compression to Mbar pressures, both in cylindrical magnetic experiments and planar gas-gun experiments [2][3][4]. (The gas-gun experiments actually employed a series of small shocks to ring-up the sample to the required pressure.) Magnetic fields in excess of 2 kT (equivalent to >1.6 TPa) have now been achieved [5]. However, up to 1998 these pulsed, high pressure magnetic compression experiments were usually performed in cylindrical geometries. Then Asay[6] reported the isentropic compression experiment (ICE), with which he obtained accurate isentropic equation of state (EOS) data at Mbar-stresses in a planar geometry by magnetic loading. A planar geometry has several advantages: the one-dimensional wave propagation into the sample under test greatly simplifies data analysis and therefore improves the accuracy of the technique; and it provides ready access to the sample, thus allowing a variety of diagnostic techniques to be used, most notably VISAR.

In the ICE experiment smoothly rising (shock-free) mechanical compression waves are propagated into various samples by electromagnetic loading in a planar geometry. Moreover, a complete EOS curve is acquired in one experiment, i.e., continuously from zero up to the peak pressure. A shock-free stress of 300 GPa has now been achieved at Sandia, and they have obtained EOS data for aluminum at

* This work was supported by the U.S. Department of Energy

250 GPa. In fact, high quality isentropic EOS data have now been obtained for many materials, e.g., copper, tantalum [7] and high explosives [8].

The Sandia team performs ICE on their Z-Accelerator, which is a 4-MV Marx machine, designed to provide current pulses up to 20 MA in risetimes of ~100 to 500 ns. Many research laboratories now use the Z-machine to routinely obtain EOS data on their own materials, and a few groups have been developing their own ICE machines. Notably the French have developed a relatively small capacitor bank system (GEPI) designed to provide ICE-EOS data up to 100 GPa and high velocity flyer plates [9], and we at the Los Alamos National Laboratory (LANL) are developing the HEPP-ICE system, described here.

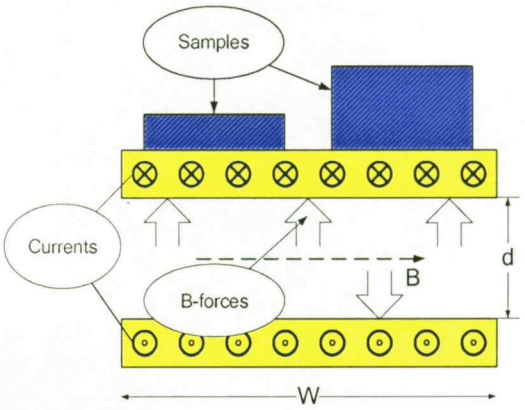

Figure 1. B-forces between conductors apply isentropic pressure to two samples. Crosses and dots indicate current flow.

TECHNIQUE

Electromagnetic principles of ICE

The basic principle of ICE is the isentropic magnetic loadings of two or more identical samples of different thicknesses, situated on the rear surfaces of a pair of parallel conductors, see Figure 1. These samples may be used as both the conductors and the material under test. In the case of HEPP-ICE,[10] consider two equal and opposing currents (I) flowing in two flat and parallel conductors of equal width (W) and separated by a small distance (d). The magnetic stresses (B-forces) on the inside surfaces is given by the vector product $\mathbf{P_B} = \mathbf{J} \times \mathbf{B}$, where J is the current per unit width. In the simplest case when W>>d, and J is uniform, equal and opposite in the electrodes, the magnetic field on the inside surface of one conductor due the current in the opposing surface is $\frac{1}{2}\mu_0$ J.[11] Then the stress normal to the inside surfaces $\mathbf{P_B} = \mathbf{J} \times \mathbf{B} = \frac{1}{2}\,\mu_0 J^2$. If $J = 10^9$ A/m for example, then $P_B = 200\pi$ GPa (6.28 Mbar). If the time of application of these currents is short, compared to the time it takes a compression wave to traverse the conductor and back again, then high pressures can be reached before the conductors have time to move apart. In the ICE experiments the currents risetimes are typically ~300 to 600 ns.

Departures from uniform sample loading.

$$B_1(y) = \tfrac{1}{2}\mu_0 J_2 \times \frac{1}{\pi}\left\{\operatorname{atan}\left(\frac{W/2 - y}{d}\right) + \operatorname{atan}\left(\frac{W/2 + y}{d}\right)\right\} \qquad (1)$$

As the B-forces are sustained (and the stresses greatly exceeding the material strength) the inside surfaces are forced apart, d/W increases and the W>>d condition is eventually violated. Then the B-field, current density and B-forces become distorted (non-uniform) as follows.

If we assume that the surfaces are initially flat and parallel, and J is uniform across the width, the magnitude of the B-field at the surface of one plate, $B_1(y)$, at a distance from the center of the plate (y), due to current density J_2 in the opposite plate can be shown to be given by Equation (1) and P_B, which equals $\mathbf{J_2} \times \mathbf{B_1}$, varies with y accordingly. From Equation(1) it is seen that as d/W increases that B(y) and hence P_B become non-uniform, they are higher in the center (at y=0) and lower at the edges. This causes the electrodes to bow which in turn causes the current densities to be-

come non-uniform. Moreover, at these very high current densities and relatively fast risetimes the currents are confined to the skin depth, and this thin layer (~1 mm in copper at typical ICE current densities and risetimes) can melt or ablate. Also, the initial current density is often not uniform across the width, e.g., because a tapered conductor feeds current to the electrode causing higher current densities at the edges. Consequently, all these combined processes have no simple analytic description and can only be solved by 3-D computer hydrocodes with coupled MHD capabilities, see Goforth.[12] Fortunately, an accurate knowledge of the magnetic forces is not necessary to obtain accurate EOS data because the magnetic fields of opposing conductors mirror each other exactly. Consequently, identical forces are applied to the two opposing surfaces under test and EOS data may be obtained to well within 1% accuracy, as will be seen later.

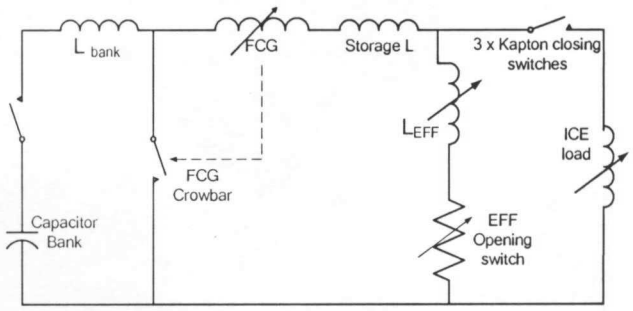

Figure 2. Basic HEPP-ICE circuit.

HEPP-ICE circuit.

Most of the components in the HEPP-ICE system existed prior to ICE and have been adapted from other applications. However, for predictable performance and control of the current profile, HEPP-ICE requires a timing precision of ~50 ns, which is better than is normally achieved with an HEPP system. Kapton (polyimide) closing switches were developed that combine low time jitter (50 ns), insensitivity to applied voltage (-0.5 ps/V), and a small electrical impedance (<1 nH) [13]. A 6 mF, 20 kV capacitor bank provides a seed current of ~2 MA to a 4-in×5-in plate flux compressor [14][15], the FCG in Figure 2. The FCG transfers up to 12 MA into a storage inductor of ~25 nH and an explosively-formed fuse (EFF) opening switch[16]. Three parallel explosively-driven Kapton closing switches then transfer current to the load at the appropriate time. This circuit is capable of delivering 7 MA (dI/dt ~3 $\times 10^{13}$ A/s) into loads of 1 to 2 cm width with the required risetimes and will produce isentropic compression at pressures in the range of 0 to 250 GPa. Goforth[12] showed that a similar but larger HEPP system is capable of producing ~1.7 TPa shock-free loading in 2-mm thick samples.

Circuit modeling of HEPP-ICE

For experimental design and subsequent data analysis we need accurate predictive models of the system performance. The explosive components and load are time dependent, and the load is also current dependent, so accurate models had to be developed for each. The plate generator (FCG) was modeled using tables of inductance vs. time, L(t), and rate of change of inductance versus time, dL(t)/dt derived from experimental data. The EFF model was a combination of an experimental resistance versus time relationship, R(t), and a calculated inductance model for L(t) and dL(t)/dt. Both of these models (FCG and EFF) can be predetermined before modeling. However, the load inductance increases with time as the B-forces increase the separation, d, so we must calculate both its L(t) and dL(t)/dt dynamically during the circuit calculation. Previously we had solved this by combining separate circuit and hydrocode calculations in an iterative process. We have now built a SPICE circuit model that incorporates all the physics of the load to a first order approximation. The model calculates: the B-forces according to Equation(1); d as a

function of the B-forces and the acoustic wave interactions; and L(t) according to Equation(2) where K is an analytic solution for the correction factor for separation[17] and *l* is the length of the conductors. Diffusion is calculated as a separate dynamic resistance as if the current flows in a sheet of metal of thickness equal to the skin depth[18]. All these separate models have been incorporated into one SPICE circuit, which allows for rapid and accurate predictions of ICE performance.

$$L(t) = \frac{\mu_0 l d(t)}{W} \cdot K\left(\frac{d}{W}\right) \quad (2)$$

Lagrangian and Backward data analysis

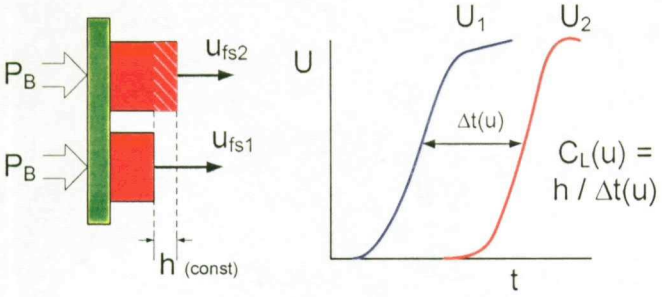

Figure 3. Left: VISAR velocities recorded on rear surfaces of samples. Right: Two particle velocity records used to calculate $C_L(u)$.

Two samples, with a difference in thickness of h, are compressed by the same B-forces and we measure the particle velocity profiles, u(t), at the rear surfaces, with or without windows, Figure 3. Using Lagrangian wave analysis [19] we calculate the sound speed $C_L(u)$ for the wave profiles to travel a distance h at each value of u(t) in time as shown. The differential form of the momentum conservation, Equation(3), is then used to calculate the change in stress, $d\sigma$, for each step of particle velocity, du, going up the curve u(t), where ρ_0 is the initial density (at zero stress). In this way we can calculate continuous EOS relationships between stress, sound speed, particle velocity, and density from 0 to the peak stress.

$$d\sigma = \rho_0 c_L(u) du \quad (3)$$

A recent development in ICE data analysis is the "Backward" technique developed by Hayes[20]. Because the data are isentropic, i.e., there are no discontinuities in the wave profiles, it is possible to calculate backwards in space from the rear faces of the samples to the inside surfaces driven by the magnetic loading. The technique depends on the fact that the stresses at the inside surfaces are equal. If the calculations are performed with the correct EOS then the calculated pressures must match. Hayes makes an initial estimate of the EOS in polynomial form, then iterates on the polynomial until an exact match is found. The application of these techniques to experimental data is shown in the next section.

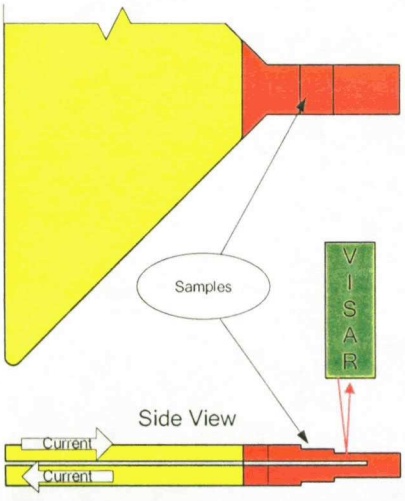

Figure 4. Load: Top and side views.

Experimental results

The load section with four copper samples is shown in Figure 4. The load section comprised a brass transmission line (tapered to minimize inductance) converging from 30 cm to a width of 4 cm, and a copper load section tapering to 1.27 cm width. The conductors were separated by 660-μm gap and insulated with Kapton sheets (not shown). Four stepped copper samples, each 12.7 mm wide, were mounted in the load section with thicknesses between 1.79 and 2.52 mm. Particle velocities were measured with VISARs at the back face of

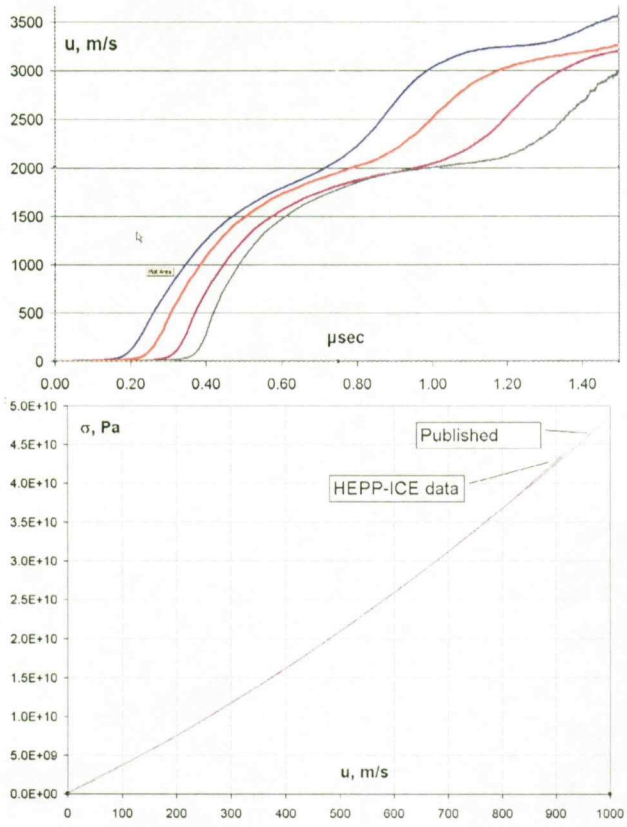

Figure 5. a) Raw VISAR velocity data and b) isentropic EOS results

each sample (which was evacuated to eliminate air flash). Figure 5 shows the raw VISAR data (a) and the isentropic EOS results (b), derived from the Lagrangian analysis above. The EOS results are for all four samples, and there is agreement to within 0.2% of each other in stress (the curves lay on top of one another). The published isentrope[21] is also shown, and it passes through the results (within 0.2%) up to 40 GPa.

Figure 6 shows the stresses at the inside surfaces obtained with the backward analysis. The same published isentrope was used to perform these calculations. The agreement between each pair is within 0.2% in stress, but the stresses for the two sets of samples differ significantly. The top pair of curves is for the thinner samples near the top of the load. We believe this is due to current density being higher along the edges of the lower samples, because of the tapered electrode design.

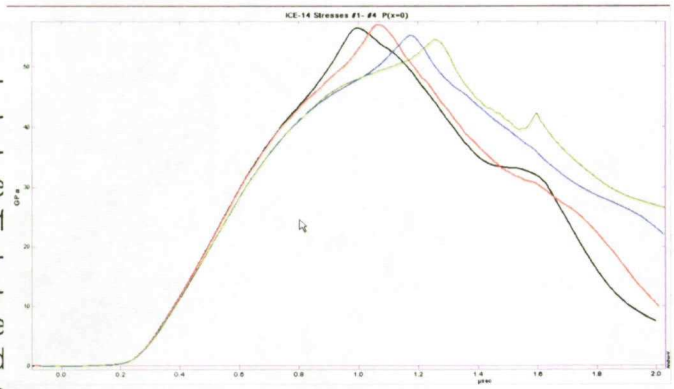

Figure 6. Results of Backward calculations for the two sets of samples.

DISCUSSION

Backward analysis. There is evidence from the backward calculations that the tapered electrode design forces the current density to be higher along the outside edges of the lower samples (nearer the taper) and therefore lower at the center. The agreement between the two sets of curves in the backward calculation suggests that there is an exact mirror imaging of the B-fields on opposing sample faces. The technique has proven to be extremely useful not only in EOS data analysis, but also in understanding the operation of the HEPP-ICE system. For example, we have identified the effects of current non-uniformities, and other experimental artifacts. There is still much work to be done to deal with such issues as phase changes in the backward analysis.

Design issues. At the beginning of the HEPP-ICE program we struggled with a number of issues that prevented us from obtaining the correct load-current profile. We systematically eliminated various problems, most notably to do with insulation, corona, and the closing switches. Having identified and corrected these problems,

we have now successfully fired six such experiments in succession and obtained the correct current profiles each time. There are still many things we wish to improve, e.g., the time jitter of the EFF switch and the accuracy of sample measurement.

SUMMARY

We have demonstrated the HEPP version of the ICE technique can be used to obtain accurate (within 0.2% in stress) isentropic EOS data at Mbar stresses, and that the system is reliable, reproducible and predictable. The technique has be used to obtain accurate EOS data for OFHC copper up to 45 GPa, but can easily be extended to reach stresses of ~250 GPa with the prototype system and 1.7 TPa with an advanced system[12].

REFERENCES

[1] Fowler, C.M., et al., "Nearly Isentropic Compression of Materials by Large Magnetic Fields : A Survey," *Procs. of.Intl. Symp. on Intense Dynamic Loading and Its Effects,* Chengdu, China, June 92.
[2] Nellis, W.J. and Mitchell, A.C., *Shock Comp. of Condensed Matter – 1997,* p.13.
[3] Fortov, V.E., et al., *Shock Comp. of Condensed Matter – 1999,* Am. Inst. Phys., p.49.
[4] Veeser, L.R., et al., *Proc. 8th Intl. Conf. on Megagauss Field Generation and Related Topics, Oct 1998..*
[5] Dolotenko, M., *Proc. 8th Intl. Conf. on Megagauss Field Generation and Related Topics, Oct 1998.*
[6] Asay, J.R., *Shock Comp. of Condensed Matter – 1999,* Am. Inst. Phys., p.261.
[7] D.B. Reisman, *JAP,* 89(3), p.1625, 1 Feb. 2001.
[8] D.B. Reisman, "*Proc. APS Shock Comp. of Condensed Matter,* June 2001, Atlanta, GA.
[9] G. Avrillaud et al., "*Proc. 14th IEEE Intl. Pulsed Power Conference, Dallas,* TX, p.913.
[10] The Z-machine has concentric electrodes but similar relationships apply.
[11] All formulae are in SI units.
[12] J.H. Goforth, *Proc. 9th Intl. Conf. on Megagauss Field Generation and Related Topics,* July 2002.
[13] D.G. Tasker, *Proc. 9th Intl. Conf. on Megagauss Field Generation and Related Topics,* July 2002.
[14] D.J. Erickson, "Design of Foil Implosion System for Pioneer I Experiments," Proc. Fifth IEEE Pulsed Power Conference, June 10-12, 1985.
[15] J.H. Goforth, "Five to 10 MA Experiments using Flat Plate Explosive Generators," Proc. PPPS-2001, IEEE Pulsed Power Plasma Science conference, June 17-22, 2001, p.150.
[16] Tasker, D.G, Proc. 8th Intl. Conf. on Megagauss Magnetic Field and Related Topics, Oct. 1998, Tallahassee, FL.
[17] Knoepfel, H.E., "Magnetic Fields," John Wiley & Sons Inc., 2000, p.369.
[18] Knoepfel, "Magnetic Fields," Chapter 4.
[19] Aidun, J.B., and Gupta, Y.M., JAP, 43, 4669 (1972).
[20] Hayes, D., "Backward Integration of the Equations of Motion ... ," Sandia National Labs., SAND2001-1440, May 2001
[21] "Selected Hugoniots," Los Alamos Scientific Laboratory, May 1, 1969, LA-4169-MS.